Journal of Crystal Growth 323 (2011) 187–190

Contents lists available at ScienceDirect

Journal of Crystal Growth

journal homepage: www.elsevier.com/locate/jcrysgro

# Growth and annealing of InAs quantum dots on pre-structured GaAs substrates

M. Helfrich [a], D.Z. Hu [a], J. Hendrickson [b], M. Gehl [b], D. Rülke [a], R. Gröger [c], D. Litvinov [d], S. Linden [e], M. Wegener [a], D. Gerthsen [d], T. Schimmel [c], M. Hetterich [a], H. Kalt [a], G. Khitrova [b], H.M. Gibbs [b], D.M. Schaadt [a,*]

[a] DFG-Center for Functional Nanostructures (CFN) and Institut für Angewandte Physik, Karlsruhe Institute of Technology (KIT), 76131 Karlsruhe, Germany
[b] College of Optical Sciences, University of Arizona, Tucson, AZ 85721, USA
[c] Institute of Nanotechnology (INT) and Institut für Angewandte Physik, Karlsruhe Institute of Technology (KIT), 76131 Karlsruhe, Germany
[d] Laboratorium für Elektronenmikroskopie (LEM), Karlsruhe Institute of Technology (KIT), 76131 Karlsruhe, Germany
[e] Physikalisches Institut, University of Bonn, 53115 Bonn, Germany

ARTICLE INFO

Available online 10 December 2010

*Keywords:*
A1. Quantum dots
A1. Site-selective growth
A1. Patterning
A1. *In situ* annealing
A3. Molecular beam epitaxy

ABSTRACT

In this study, we investigated the effect of *in situ* annealing on InAs quantum dots site-selectively grown on pre-structured GaAs substrates. A morphological transition is observed with original double dots merging into one single dot during annealing. This is accompanied by a reduction of quantum dots originally nucleating between defined sites. The photoluminescence intensity of annealed site-selective quantum dots is compared to annealed self-assembled dots with linewidths of single dot emission of about 170 and 81 μeV, respectively. UV-ozone cleaning is used to optimize the sample cleaning prior to quantum dot growth.



## 1. Introduction

Semiconductor quantum dots (QDs) have attracted a lot of attention due to their unique properties during the past two decades. Not only do they exhibit a delta-function-like density of states, which makes them interesting for laser applications, but moreover they can generate entangled photon pairs and act as single photon sources and are thus promising candidates for quantum information schemes [1,2]. Early on, QDs were grown by self-assembly [3]. Properties, such as dot sizes or dot densities, can be altered by choosing the proper growth parameters [4]. However, this alone does not provide any control over quantum dot positions, since self-assembly is inherently a random process. With regard to quantum information applications it is essential to have an ability to define arbitrary device architectures, i.e. to control the location of each individual QD with the prospect of scalability. But not solely applications generate a desire to control QD nucleation sites. Experiments with single QDs to study their physical properties, especially coupling to cavities, require physical access to single dots, which is generally accompanied by a tedious search for the right dot.

Techniques to precisely position QDs have therefore been elaborated in the past. Top-down techniques such as electron beam lithography (EBL), local oxidation or mechanical nano-indentation have proven to be viable in order to define QD nucleation sites [5–7]. Common to those approaches is the creation of small holes on the substrate surface, which leads to selective QD nucleation at the desired locations. Pre-structuring is commonly performed *ex situ* and usually involves several process steps. Besides intended surface manipulation, contamination can occur. Therefore, great care has to be taken with regard to surface cleanliness prior to regrowth in order to inhibit unintended QD nucleation caused by defects. In addition, the optical properties are very sensitive to defects as well, so that site-selective QDs exhibit inferior optical quality compared to self-assembled ones. The main reason is attributed to a change of morphology at the hole site. The defects originate from the regrowth interface [8]. This obstacle is often circumvented by growing QD stacks consisting of a QD seed layer and a spacer layer as large as possible [9]. Reducing the dot density and controlling the occupation number of QDs per site was, however, not improved that way.

A different approach to access the aforementioned quantities makes use of the fact that QDs undergo morphological changes during annealing. At lower temperatures they tend to ripen whereas they dissolve at higher temperatures [10,11]. By choosing the right annealing conditions it should therefore be possible to control, to some extent, the final QD size as well as the QD distribution and the occupation number per site. Annealing studies on unstructured substrates have already confirmed an increase in QD size uniformity [12,13].

* Corresponding author. Tel.: +49 721 608 3893; fax: +49 721 608 4950.
*E-mail address:* daniel.schaadt@kit.edu (D.M. Schaadt).

0022-0248/$ - see front matter © 2010 Elsevier B.V. All rights reserved.
doi:10.1016/j.jcrysgro.2010.11.162

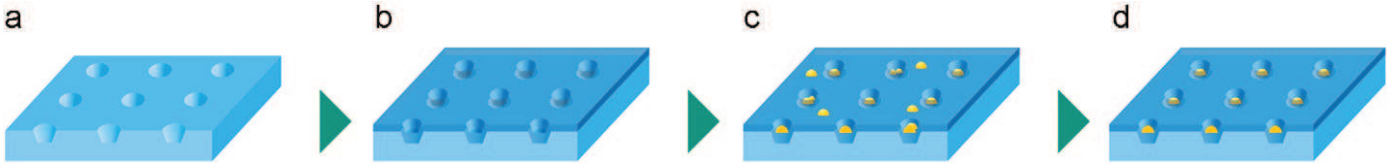


**Fig. 1.** Concept for improved site-selective quantum dot growth. In the first step a GaAs substrate is pre-structured by lithographic techniques to define nano-holes (a). The native oxide is removed and a thin GaAs buffer layer is grown on top of the pre-structured surface (b). This is followed by InAs QD growth (c). *In situ* annealing is then used to control the QD distribution and the occupation number of QDs per site (d).

We introduce a new concept for optimized site-selective QD growth, which is schematically shown in Fig. 1. Site-selectivity is achieved by lithographically defining nano-holes. *In situ* annealing is then used to improve the QD distribution and the occupation number of QDs per site. Therefore, in this study, we investigated the effect of *in situ* annealing on InAs QDs site-selectively grown on pre-structured GaAs substrates. In addition, the sample preparation process was optimized in order to account for unintended QD nucleation.

## 2. Experimental

The samples were grown by molecular beam epitaxy (MBE) in a Riber Compact 21T with the samples being continuously rotated. Epi-ready (1 0 0) GaAs wafers were used as substrates and surface-patterning was performed on top of a 90 nm GaAs epitaxial layer. Conventional electron-beam lithography was used to define 50–70 nm wide holes in a PMMA/MA (polymethyl methacrylate/methacrylate) co-polymer resist on the surface. The holes were arranged on square grids with varying lattice constants. They were etched 30 nm deep into the substrate by wet chemical etching (WCE) using $H_2SO_4$:$H_2O_2$:$H_2O$. The resist was removed and the samples were cleaned in a series of solvent baths before being heated up to 130 °C for 1 h in the load lock chamber of the MBE system in order to get rid of volatile surface contamination.

The surface oxide was removed *in situ* by Ga-assisted deoxidation [14]. Therefore, the samples were heated up to 480 °C and exposed to a low Ga-flux of ~1 ML/min. Every 30 s of Ga-exposure was followed by a pause of 30 s such that the converted $Ga_2O$ more easily desorbs from the surface. A total amount of 8 ML of Ga was provided before the substrate temperature was increased to 550 °C and the samples were annealed for 2 min under $As_4$-atmosphere. A 16 nm GaAs buffer layer (BL) was then grown at 500 °C followed by deposition of InAs at the same temperature. The growth rates for GaAs and InAs were determined as 0.3 and 0.07 ML/s with III/V beam equivalent pressure (BEP) ratios of 1:10 and 1:100, respectively. *In situ* annealing was performed right after QD growth. The samples were kept at growth temperature for different time periods and either rapidly cooled down to room temperature by switching off the substrate heater or capped with 80 nm GaAs. The uncapped samples were characterized by atomic force microscopy (AFM) whereas the capped samples allowed for transmission electron microscopy analysis and micro-photoluminescence (μ−PL) measurements, which were performed at 20 K with a He:Ne laser using a Si charge coupled device detector. The laser spot size was about 1 μm.

## 3. Results and discussion

### 3.1. *In situ* annealing of site-selective QDs

Site-selective QDs were annealed and compared to as grown site-selective ones. Fig. 2 shows a set of QD samples with both containing 1.7 ML of InAs. The as grown sample shows

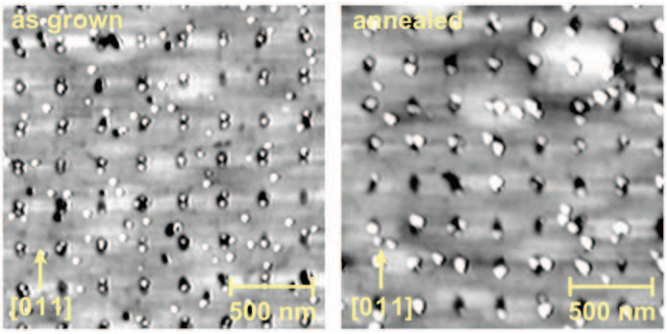


**Fig. 2.** Atomic force microscopy images of site-selective InAs QDs (1.7 ML) as grown (left) and annealed for 2:30 min (right). The gray scale is 18 nm in both cases.

predominant double dot nucleation per site. This fact is probably related to a change in hole morphology during GaAs BL growth [15]. QDs nucleating on interstitial sites (sites between holes) are found since the supplied amount of InAs is above the critical thickness for QD formation on pre-structured substrates.

After annealing the sample for 2:30 min, the number of interstitial QDs is reduced and, moreover, a morphological change of the site-selective QDs is observed. Original double dots merge into single dots. By facilitating In-adatom migration the annealing step causes the material to redistribute. The volume of the newly formed single dots is larger than the combined volume of the original double dots. This is related to the reduction of interstitial dots. The site-selective QDs appear to be more stable than the interstitial dots and ripen by collecting material from surrounding interstitial dots. This observation is best described by a kinetic model with the ripening process being limited by attachment and detachment of atoms on the dot surface [16].

The optical quality of annealed QDs was analyzed by μ−PL spectroscopy. The spectra shown in Fig. 3 were obtained from self-assembled (*blue*) and site-selective (*green*) QDs. Both samples contain 1.9 ML InAs and were annealed for 2:30 min. The intensity of the QD emission in the pre-structured sample is reduced compared to the self-assembled QDs and not all emission lines seem to fully emerge. As seen from two individual peaks (both show maximum intensity of each spectrum), the maximum intensities differ by a factor of 2. The linewidth of these QD emission peaks is 170 and 81 μeV (each full width at half maximum, FWHM) for the site-selective and self-assembled QDs sample, respectively.

μ−PL data on conventional self-assembled QDs show linewidths down to a few μeV [17]. However, these values stem from resonant excitation experiments at 2 K. Only limited μ−PL data of annealed self-assembled QDs is presently available [18] so that it is difficult to compare the possibly large linewidth of 81 μeV. Similarly, μ−PL data of as grown site-selective QDs has been published, with linewidths down to 460 μeV [9] or even 106 μeV [19], but these works deal with QD stacks and the measurements are related to the topmost QD layer. The best value of emission for a single as grown QD layer is reported to be about 500 μeV [8].

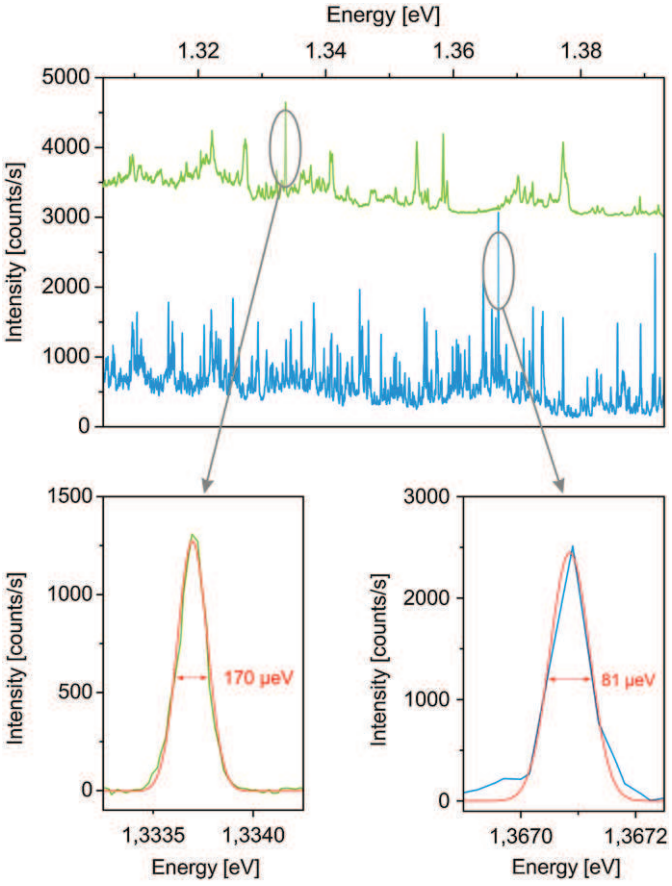


**Fig. 3.** Micro photoluminescence spectra of self-assembled (bottom) and site-selective (top) QDs. A total amount of 1.9 ML InAs was grown followed by 2:30 min annealing. The upper spectrum is offset by 3000 counts/s. Single emission peaks were extracted from the spectra showing linewidths of site-selective (left) and self-assembeld (right) QDs. The single peaks are background corrected data fitted with a Gaussian.

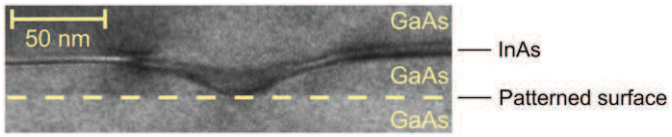


**Fig. 4.** Transmission electron microscopy image of an overgrown defect hole. The regrowth interface is indicated by the dashed line.

With regard to the fact that site-selective QDs in all cases exhibit inferior luminescence compared to self-assembled ones, our data is in agreement with other works. It has to be pointed out, though, that it is not possible to discriminate between emission coming from site-selective QDs and the one emerging from interstitial QDs. This obstacle will be addressed in follow-up experiments. Nevertheless, in comparison with previous data (not shown here) we see evidence that at least half of the site-selective QDs are optically active. A rough analysis of the above spectra yields 100 peaks with an average FWHM of $570 \pm 270$ μeV for the pre-structured sample and 170 peaks with an average FWHM of $280 \pm 110$ μeV for the self-assembled sample.

### 3.2. *Sample preparation procedure: problems and optimization*

Besides pre-defined holes additional defect holes are observed in the pre-structured area, as can be seen in Fig. 2. An overgrown defect hole is found in the TEM image of Fig. 4. Local contamination of the pre-structured surface hindered proper regrowth of the GaAs BL. However, InAs nucleates at this particular location allowing for a smooth overgrowth of the defect hole. Such unintended holes can act as nucleation sites and therefore interfere with the attempt to deterministically position QDs.

Two factors can account for the occurrence of such defect holes. First, incomplete removal of the native oxide could leave residual oxide compounds on the surface, which affect the proper GaAs regrowth. Second, insufficient surface cleaning after the lithography process could cause local organic contamination of the sample, which also impacts the GaAs growth. Incomplete deoxidation is rather unlikely since the defect holes are not randomly distributed. Some local areas are found with a high defect density whereas other areas seem very clean. In addition, by controlling the surface evolution during deoxidation by means of reflection high energy electron diffraction (RHEED), it is made sure that enough Ga is provided to completely remove the native oxide. Focus was therefore laid on analyzing and optimizing the cleaning procedure prior to regrowth.

Cleaning samples after EBL comprises several steps. After removing the resist the samples were cleaned with different solvents (trichlorethylene, acetone, isopropyl alcohol, methanol) in a heated ultrasonic bath. Finally, the samples were rinsed in bi-distilled water. Critical steps of the cleaning procedure are depicted in Fig. 5. The sample in Fig. 5(a) was cleaned in a series of solvent baths without ultrasonic aid. A lot of contamination is observed from the AFM image (large particles appearing white). The cleaning is improved by performing the whole procedure in an ultrasonic

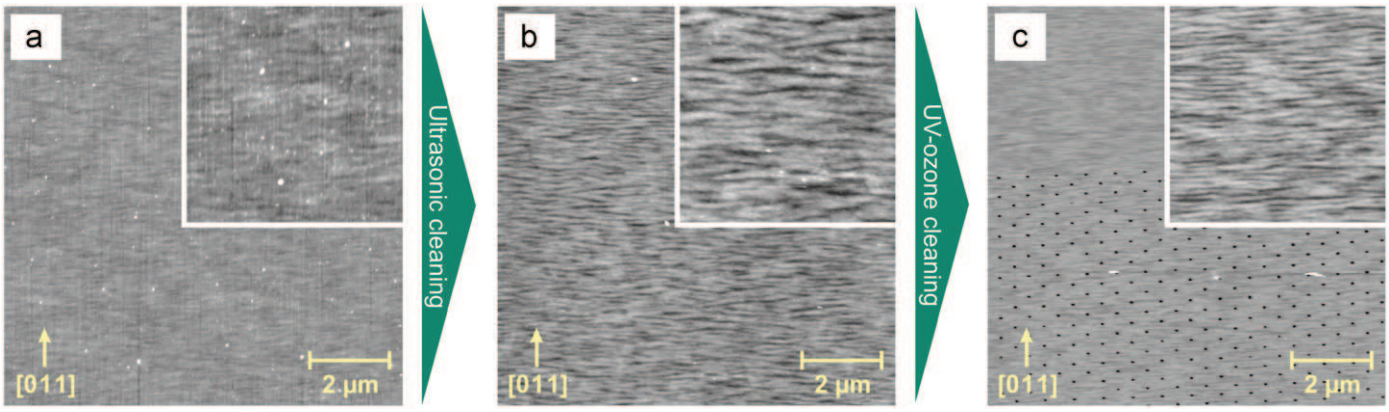


**Fig. 5.** Atomic force microscopy images of samples at different stages of the cleaning procedure: after cleaning with solvents (a), using a heated ultrasonic bath (b) and after UV-ozone cleaning (c). The pre-structured area is visible in (c). All samples were prepared in the same way. The insets are 3μm × 3μm. The gray scale is for the full size 20, 27, 58 nm and for the inset 13, 6, 4 nm in (a), (b), (c), respectively.

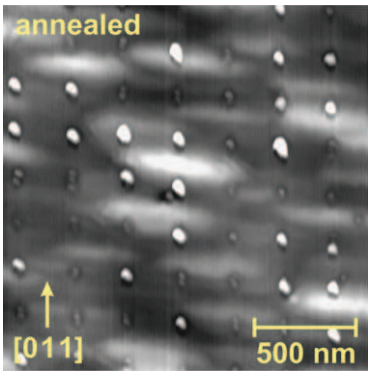


**Fig. 6.** Atomic force microscopy image of site-selective QDs. A total amount of 2.6 ML of InAs was provided followed by a 7:30 min annealing. The gray scale is 30 nm.

bath. However, small amounts of organic contamination remain on the surface, see Fig. 5(b). In order to also remove these, a UV-ozone cleaning is introduced [20]. The UV light creating and destroying ozone at the same time constantly provides atomic oxygen that reacts with organic molecules on the sample surface. Simpler, volatile compounds are formed that readily desorb. The effect is displayed in Fig. 5(c) where essentially all contamination has disappeared.

The success of the optimized sample preparation is confirmed by Fig. 6, which depicts a sample with site-selective QDs that were annealed for 7:30 min. A total amount of 2.6 ML InAs were grown prior to annealing. No defect holes are observed in the pre-structured area. In addition, no interstitial dots are found, which is ascribed to the elongated annealing time. The same morphological transition as described in the previous section is observed once more.

## 4. Conclusion

In conclusion, we have introduced a new concept for optimized growth of site-selective quantum dots. *In situ* annealing was used to control the QD distribution and the occupation number of QDs per site. A morphological transition was observed with originally two dots merging into a single dot. In photoluminescence measurements we found linewidths of annealed site-selective QDs and self-assembled QDs of 170 and 81 μeV. The cleaning process prior to regrowth was optimized by making use of a UV-ozone process. As a result, the samples are essentially free of organic contamination.

## Acknowledgments

The Karlsruhe researchers acknowledge financial support from the Deutsche Forschungsgemeinschaft (DFG) and the State of Baden-Württemberg through the DFG-Center for Functional Nanostructures (CFN) within subproject A2.6. The Tucson group would like to acknowledge support (EEC-0812072) from the National Science Foundation (NSF) through the Engineering Research Center for Integrated Access Networks (CIAN) and Atomic Molecular and Optical Physics (AMOP) and Electronics, Photonics and Device Technologies (EPDT), as well as AFOSR, and Arizona Technology & Research Initiative Funding (TRIF).

## References

[1] P. Michler, A. Kiraz, C. Becher, W.V. Schoenfeld, P.M. Petroff, L. Zhang, E. Hu, A. Imamoğlu, A quantum dot single-photon turnstile device, Science 290 (2000) 2282–2285.
[2] N. Akopian, N.H. Lindner, E. Poem, Y. Berlatzky, J. Avron, D. Gershoni, B.D. Gérardot, P.M. Petroff, Entangled photon pairs from semiconductor quantum dots, Phys. Rev. Lett. 96 (2006) 130501–130504.
[3] D. Leonard, K. Pond, P.M. Petroff, Critical layer thickness for self-assembled InAs islands on GaAs, Phys. Rev. B 50 (1994) 11687–11692.
[4] N.N. Ledentsov, V.A. Shchukin, D. Bimberg, V.M. Ustinov, N.A. Cherkashin, Yu.G. Musikhin, B.V. Volovik, G.E. Cirlin, Zh.I. Alferov, Reversibility of the island shape, volume and density in Stranski-Krastanow growth, Semicond. Sci. Technol. 16 (2001) 502–506.
[5] S. Jeppesen, S. Miller, S. Hessman, B. Kowalski, I. Maximov, L. Samuelson, Assembling strained InAs islands on patterned GaAs substrates with chemical beam epitaxy, Appl. Phys. Lett. 68 (1996) 2228–2230.
[6] O.G. Schmidt, S. Kiravittaya, Y. Nakamura, H. Heidemeyer, R. Songmuang, C. Müller, N.Y. Jin-Phillipp, K. Eberl, H. Wawra, S. Christiansen, H. Gräbeldinger, H. Schweizer, Self-assembled semiconductor nanostructures: climbing up the ladder of order, Surf. Sci. 514 (2002) 10–18.
[7] P. Atkinson, M.B. Ward, S.P. Bremner, D. Anderson, T. Farrow, G.A.C. Jones, A.J. Shields, D.A. Ritchie, Site control of InAs quantum dot nucleation by ex situ electron-beam lithographic patterning of GaAs substrates, Physica E 32 (2006) 21–24.
[8] P. Atkinson, O.G. Schmidt, S.P. Bremner, D.A. Ritchie, Formation and ordering of epitaxial quantum dots, C. R. Phys. 9 (2008) 788–803.
[9] T.J. Pfau, A. Gushterov, J.P. Reithmaier, I. Cestier, G. Eisenstein, E. Linder, D. Gershoni, Site-controlled InAs quantum dots grown on a 55 nm thick GaAs buffer layer, Appl. Phys. Lett. 95 (2009) 243106–243108.
[10] H. Lee, R.R. Lowe-Webb, W. Yang, P.C. Sercel, Formation of InAs/GaAs quantum dots by molecular beam epitaxy: reversibility of the islanding transition, Appl. Phys. Lett. 71 (1997) 2325–2327.
[11] C. Heyn, Stability of InAs quantum dots, Phys. Rev. B 66 (2002) 075307–075310.
[12] D.M. Schaadt, S. Krauss, R. Koch, K.H. Ploog, Stress evolution during growth of bilayer self-assembled InAs/GaAs quantum dots, Appl. Phys. A 83 (2006) 267–269.
[13] D.Z. Hu, A. Trampert, D.M. Schaadt, Morphology and stress evolution of InAs QD grown and annealed in-situ at high temperature, J. Cryst. Growth 312 (2010) 447–451.
[14] P. Atkinson, S. Kiravittaya, M. Benyoucef, A. Rastelli, O.G. Schmidt, Site-controlled growth and luminescence of InAs quantum dots using *in situ* Ga-assisted deoxidation of patterned substrates, Appl. Phys. Lett. 93 (2008) 101908–101910.
[15] S. Kiravittaya, H. Heidemeyer, O.G. Schmidt, In(Ga)As quantum dot crystals on patterned GaAs (0 0 1) substrates, in: O.G. Schmidt (Ed.), Lateral Alignment of Epitaxial Quantum Dots, Springer, Berlin, 2007, pp. 489–511.
[16] D.Z. Hu, D.M. Schaadt, K.H. Ploog, Stress development during annealing of self-assembled InAs/GaAs quantum dots measured in situ with a cantilever beam setup, J. Cryst. Growth 293 (2006) 546–549.
[17] M. Bayer, A. Forchel, Temperature dependence of the exciton homogeneous linewidth in $In_{0.60}Ga_{0.40}As$/GaAs self-assembled quantum dots, Phys. Rev. B 65 (2002) 041308.
[18] D.Z. Hu, Stress evolution during growth of InAs on GaAs measured by an in-situ cantilever beam setup, Dissertation, Humboldt-Universität zu Berlin 〈http://nbn-resolving.de/urn:nbn:de:kobv:11-10077303〉, 2007.
[19] C. Schneider, A. Huggenberger, T.S. Sünner, T. Heindel, M. Strauß, S. Göpfert, P. Weinmann, S. Reitzenstein, L. Worschech, M. Kamp, S. Höfling, A. Forchel, Single site-controlled In(Ga)As/GaAs quantum dots: growth, properties and device integration, Nanotechnology 20 (2009) 434012.
[20] S.I. Ingrey, Surface Processing of III–V Semiconductors, in: P.H. Holloway, G.E. McGuire (Eds.), Handbook of Compound Semiconductors, Noyes Publications, Park Ridge, NJ, 1995, pp. 251–284.